Biochimica et Biophysica Acta 1784 (2008) 1771-1776

Contents lists available at ScienceDirect

Biochimica et Biophysica Acta

journal homepage: www.elsevier.com/locate/bbapap

Replacement of the active surface of a thermophile protein by that of a homologous mesophile protein through structure-guided 'protein surface grafting'

Divya Kapoor [a], Vijay Kumar [a], Sanjeev K. Chandrayan [a], Shubbir Ahmed [a], Swati Sharma [a], Manish Datt [b], Balvinder Singh [b], Subramanian Karthikeyan [a,*], Purnananda Guptasarma [a,c,*]

[a] Division of Protein Science and Engineering, Institute of Microbial Technology, Chandigarh 160 036, India
[b] Division of Bioinformatics, Institute of Microbial Technology, Chandigarh 160 036, India
[c] Adjunct Faculty, Department of Biology, Indian Institute of Science Education and Research, Chandigarh 160 019, India

ARTICLE INFO

Article history:
Received 28 March 2008
Received in revised form 10 May 2008
Accepted 13 May 2008
Available online 13 June 2008

Keywords:
Protein surface grafting
Protein activity remodeling
Protein stability remodeling
Beta sheet remodeling
Protein folding and stability

ABSTRACT

Using several tens of rationally-selected substitutions, insertions and deletions of predominantly non-contiguous residues, we have remodeled the solvent-exposed face of a beta sheet functioning as the substrate-binding and catalytically-active groove of a thermophile cellulase (*Rhodothermus marinus* Cel12A) to cause it to resemble, both in its structure and function, the equivalent groove of a mesophile homolog (*Trichoderma reesei* Cel12A). The engineered protein, a mesoactive–thermostable cellulase (MT Cel12A) displays the temperature of optimal function of its mesophile ancestor and the temperature of melting of its thermophile ancestor, suggesting that such 'grafting' of a mesophile-derived surface onto a thermophile-derived structural scaffold can potentially help generate novel enzymes that recombine structural and functional features of homologous proteins sourced from different domains of life.

1. Introduction

Protein engineering has been used to manipulate the structural and functional properties of proteins using a variety of different approaches, including rational mutagenesis [1–5], combinatorial mutagenesis coupled with directed evolution [6–9], hybrid rational–combinatorial approaches [10–12], and domain fusion/swapping approaches [13,14], with comparable rates of success, or failure, characterizing each of these approaches [15]. Here, we describe a novel structure-guided mutagenesis-based engineering approach that we call 'protein surface grafting'. Functionally, this method is akin to domain fusion/swapping; operationally, however, it involves the swapping (between structurally-homologous proteins) of surfaces made up of several tens of non-contiguous residues brought together through chain folding, rather than entire protein domains comprising contiguous stretches of sequence. Our objective in developing this method has been to facilitate rational genetic recombination of the interior of a protein with the surface of a different (structurally-homologous) protein, to combine the structural stability of the former with the functional characteristics of the latter.

To perform a 'proof-of-concept' demonstration of this approach, we selected two structurally-homologous, single domain, endoglucanases (cellulases) of beta jelly-roll fold structure, displaying a high level of polypeptide backbone atom superimposability (1.1 Å RMSD) but low overall sequence identity (~28%). One of these proteins is TR Cel12A (PDB ID 1OA2) from the mesophile fungus, *Trichoderma reesei* [16]. The other, homologous protein, is RM Cel12A (PDB ID 1H0B) from the thermophile bacterium, *Rhodothermus marinus* [17]. These proteins differ in their temperatures of optimal function (T_{opt}) and structural melting (T_m). The T_{opt} of TR Cel12A is 50 °C [18], while that of RM Cel12A is 90 °C [19]. Similarly, the T_m of TR Cel12A is 54 °C [20], while that of RM Cel12A is ≫90 °C [17]. We picked these two proteins with a view of replacing the substrate-binding and catalytic surface of RM Cel12A with that of TR Cel12A, while retaining the interior residues of RM Cel12A, to examine whether we could generate a novel protein displaying the high structural stability of RM Cel12A and the moderate temperature of optimal function of TR Cel12A.

Structurally, both proteins consist of a single alpha helix and two stacked (twisted) beta sheets made up of identical numbers of strands (Fig. 1A). The concave solvent-exposed face of the upper sheet forms the cellulose-binding and hydrolyzing groove. Groove residues are contributed by loops connecting strands in the upper sheet, as well as by several of the strands themselves. About 60 residues at structurally-analogous positions form the floor and walls of the grooves, in both enzymes, these being predominantly non-contiguous and brought together through chain folding.

* Corresponding authors. P. Guptasarma is to be contacted at Division of Protein Science and Engineering, Institute of Microbial Technology, Chandigarh 160 036, India. Tel.: +91 172 2636680x3301; fax: +91 172 2690585. S. Karthikeyan, Tel.: +91 172 2636680x3108; fax: +91 172 2690585.
E-mail addresses: skarthik@imtech.res.in (S. Karthikeyan), pg@imtech.res.in (P. Guptasarma).

1570-9639/$ – see front matter © 2008 Elsevier B.V. All rights reserved.
doi:10.1016/j.bbapap.2008.05.007

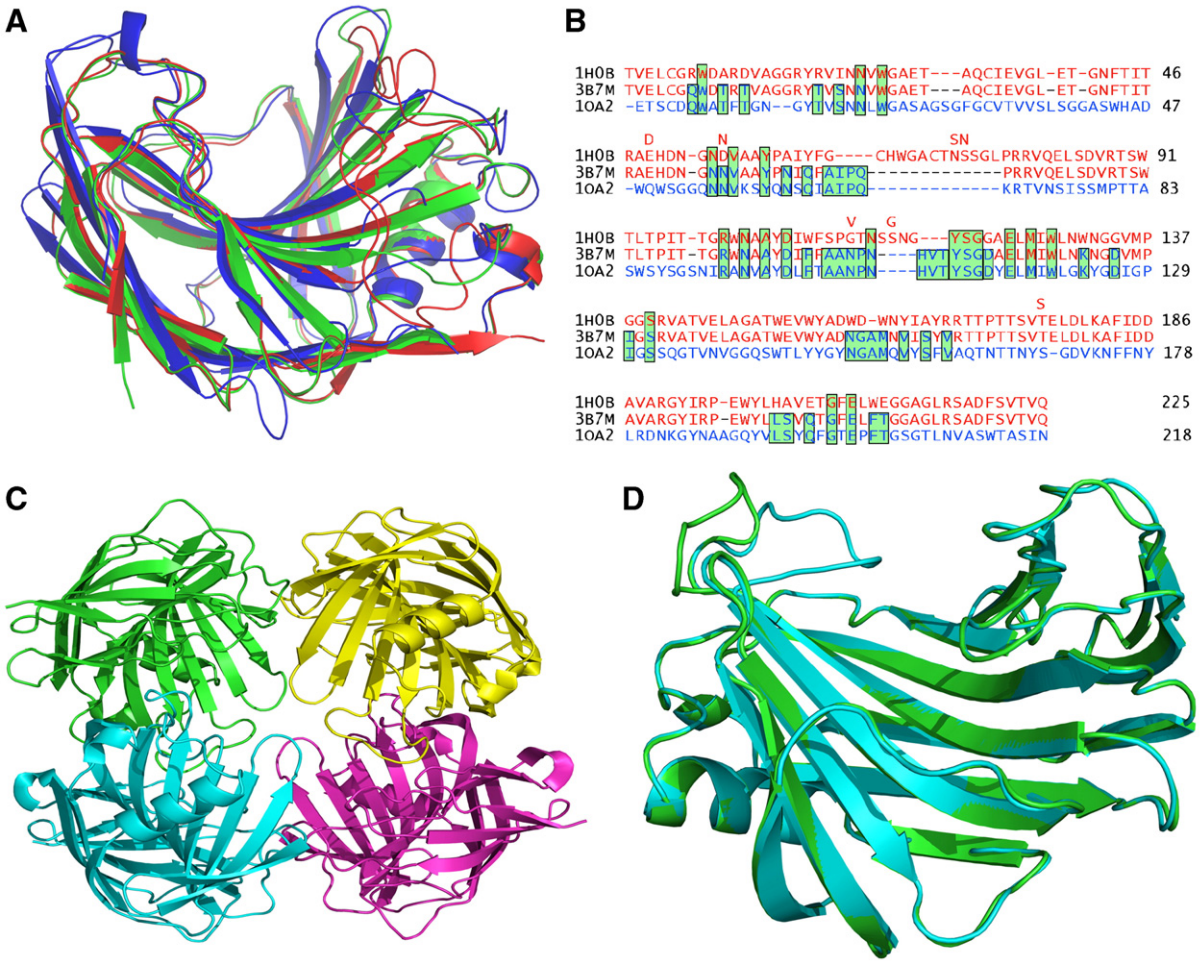

Fig. 1. Structures and structure-based sequence alignments of RM Cel12A (PDB ID 1H0B), MT Cel12A (PDB ID 3B7 M) and TR Cel12A (PDB ID 1OA2). Panel A. Ribbon diagrams of the superimposed polypeptide backbones of RM Cel12A (red), TR Cel12A (blue) and MT Cel12A (green). Panel B. Structure-based alignment of the sequences of RM Cel12A, TR Cel12A, and MT Cel12A. Groove residues with solvent-facing sidechains are highlighted by boxes in green, distinguishing conserved residues (boxes covering three rows) from non-conserved residues (boxes covering two rows). Single residues above top row indicate conflicts with the reported sequence of RM Cel12A (Supplementary Table S8). Panel C. A ribbon diagram representation of homotetrameric MT Cel12A. Panel D. A ribbon diagram showing MT Cel12A with two loop conformations in green, and cyan.

We argued that surface beta sheets in proteins must lend themselves to facile remodeling of solvent-exposed faces through transplantation, or grafting, of sidechains between structural homologs. Note that, by default, alternate residues within each strand in any solvent-exposed sheet face either the solvent, or a structure within the interior of the protein (e.g., another sheet). Therefore, the solvent- and interior-facing faces of a sheet employ different groups of sidechain–sidechain interactions, separated by the plane of the sheet, and autonomous of each other. The existence of a high degree of superimposability of backbone atoms between structurally-homologous sheets from unrelated proteins shows that different surfaces (all pre-evolved by nature) can be formed through use of the same backbone coordinates. Here, we demonstrate that the use of the same backbone coordinates by two proteins facilitates rational structure-guided transplantation of the surface residues of one with those of the other, to produce a mesoactive–thermostable hybrid enzyme, MT Cel12A.

2. Materials and methods

2.1. Protein design

The software LSQMAN [21] was used to superimpose the structures of RM Cel12A and TR Cel12A. Visual analysis was used to identify residues constituting the substrate-binding and catalytically-active groove of each protein (Supplementary Tables S1–S4); combined with the LSQMAN output, this helped to identify pairs of groove-forming residues at structurally-analogous positions in the two proteins, and to differentiate residues with solvent-facing sidechains from those with protein interior-facing sidechains. Other aspects of the design are described in the main text of the manuscript, in the Results and discussion section.

2.2. Mutagenesis and gene synthesis

We created two genes encoding the recombinant forms of the naturally-occurring RM Cel12A, and the recombinant non-naturally-occurring MT Cel12A. The scheme used for the gene syntheses is shown in Supplementary Fig. S1. The primers used for PCR splicing-by-overlap extension (SOE-PCR) are shown in Supplementary Table S5. The conditions used for the various steps of SOE-PCR are described in Supplementary Table S6. The gels showing the various amplicons prepared through the different reactions mentioned in Supplementary Table S6 are shown in Supplementary Fig.S2, with sizes of all amplicons mentioned alongside in basepairs. Gene syntheses incorporated (i) a Bam HI restriction site (flanked at its 5′ end by a 12 basepair overhang, to facilitate digestion) immediately preceding the codon encoding the starting N-terminal residue (threonine) in genes encoding both RM Cel12A and MT Cel12A, (ii) a stop codon following the codon encoding the last, C-terminal residue (glutamine), and (iii) a Hind III restriction site (flanked at its 3′ end by a 12 basepair overhang, to facilitate digestion) immediately succeeding the stop codon. The Bam HI and Hind III restriction sites were digested to allow insertion and ligation of the genes into pQE-30 (Qiagen) vectors. Besides a selection marker (ampicillin resistance), the vector provides an inducible promoter, the transcription start site, the translation start site, and an N-terminal affinity tag (N-MRGSHHHHHGS-C). The bases used in the vector to encode the last two residues of the tag, i.e., G and S, together constitute the Bam HI site, allowing insertion of the synthesized genes. The vector also provides a stop codon after the Hind III site, but we preferred to use a stop codon before the Hind III site, immediately after the C-terminal

glutamine, as already mentioned. Transformation of the ligated vectors was done into competent *Escherichia coli* XL-1 Blue cells bearing the genotype, *hsd*R17 *rec*A1 *lac*F′ [*pro*AB+*lacI*^{q} *lac*Z Δ15 Tn10 (tet^r)]. Selection of clones was done on LB plates containing tetracycline and ampicillin. An Applied Biosystems DNA sequencer (3130 XL analyzer) was used for performing automated DNA sequencing of clones. Plasmids were purified from XL-1 Blue cells using the ABI MiniPrep kit. Thermo-(cycle)-sequencing reactions were performed either with a vector-specific forward primer with the sequence 5′-CGGATAACAATTTCACACAG-3′, which was used to read through the gene regions encoding the N-terminal end of the protein, or a vector-specific reverse primer with the sequence 5′-GTTCTGAGGTCATTACTGG-3′ which was used to read through the regions encoding the C-terminal ends of the proteins. Reactions used the ABI ready reaction mix (Big Dye Terminator v3.1 cycle sequencing RR-100), with denaturation at 96 °C (5 min) followed by 30 cycles of denaturation at 96 °C (1 min), annealing at 50 °C (1 min), and extension at 60 °C (2 min). Post-reaction cleanup was done through a standard procedure incorporating washes with EDTA and ethanol, prior to loading onto the analyzer. The electrophoretogram showing the sequence of the gene encoding MT Cel12A is provided in Supplementary Fig. S3.

2.3. Protein expression and purification

Secondary cultures of XL-1 blue *E. coli* cells overexpressing MT Cel12A, set up in a total volume of 2 l in shake flasks, were grown at 37 °C up to $O.D_{600}$ of ~0.6, and induced with 0.4 mM IPTG. Harvesting of cells was done 12 h after induction. Harvested cells were lysed and subjected to standard Ni-NTA-based affinity purification under non-denaturing conditions (Qiagen), with the exception that elution was performed with 1 M imidazole. The imidazole was later dialysed out, to obtain pure folded protein. SDS-PAGE photographs showing purification are presented in Supplementary Fig. S4.

2.4. Protein characterization

Purified MT Cel12A was subjected to mass determination on a Voyager DE-STR MALDI-TOF mass spectrometer (data in Supplementary Fig. S5). For wavelength scan-based CD spectral measurements, a Jasco J-810 spectropolarimeter was used with protein concentrations in the range of 0.1–0.3 mg/ml, using cuvettes of path length 0.1 or 0.2 cm, and scanning raw ellipticity (θ) values in the range of 250 to 195 nm with N_2 gas flowing at 6–9 l/min. For standard wavelength scans, raw θ values were converted to mean residue ellipticity (MRE) values using the formula, $[\theta]=\{\theta_{obs}\times 100\times$ mean residue weight$\}/\{$concentration (mg/ml)×path length (cm)$\}$. For structure–melting temperature scans, MRE values were monitored at 217 nm between temperatures ranging from 25 °C to 98 °C, with a rate of change of temperature of 3 °C/min using a 0.2 cm path length cuvette fitted with a 0.8 cm heat-conducting metal-spacer block, and the Peltier accessory of the Jasco J-810. For gel filtration-based examination of the hydrodynamic volume and elution behavior of MT Cel12A at different concentrations (data in Supplementary Fig. S6), a pre-calibrated and appropriately pre-equilibrated micro-analytical Superdex-75 gel filtration column (bed volume is 2.4 ml), connected to a SMART chromatographic workstation (Pharmacia) was used.

2.5. Activity measurements

Activity was measured by the DNS stopping-based method [22]. For total enzyme activity measurements at a variety of temperatures (with a fixed pH of 5.0; the optimum pH of activity of TR Cel12A), or at a variety of pH values (with a fixed temperature of 50 °C; the temperature of optimal activity of TR Cel12A), the conditions detailed below were used. *Temperature scan* — For incubation at each temperature, we used a final MT Cel12A concentration of 0.1 mg/ml and NaCl concentration of 100 mM in pH 5.0 citrate buffer (final concentration 35 mM). The reaction volume was made up to 1 ml with water for each experiment, and to this 1 ml of 1.8% CMC (carboxymethyl cellulose) was added to make up a total volume of 2 ml, and the solution incubated for 60 min. A total of five such experiments were conducted for each temperature. Different tubes containing 2 ml each were incubated at the following temperatures: 10, 20, 30, 40, 50, 60, 70, 80, and 90 °C. Following incubation, 3 ml of DNS (dinitrosalicylic acid) reagent were added to each tube, and the tubes were boiled for 15 min, to generate color through the reaction of the DNS with reducing sugars liberated by the action of the cellulase on the CMC substrate. A control reaction was also incubated without enzyme. Color development was estimated by absorption measurement at 550 nm, and the value for the control (~0.03) was subtracted. The highest activity obtained was considered to be 100% and the remaining activities were converted into percentage values of the maximum activity observed. *pH scan* — For incubation at each pH, we used a final MT Cel12A concentration of 0.1 mg/ml and NaCl concentration of 100 mM in the appropriate buffer (final concentration 35 mM). Reaction volume was made up to 1 ml, and to this 1 ml of 1.8% CMC was added to make up a total volume of 2 ml, and the solution incubated for 60 min at 50 °C. A total of three such experiments were conducted for each pH. Different tubes containing 2 ml each of the above mixture were incubated at pH values ranging through 3, 4, 5, 6, 7, 8, 9, and 10. For pH ranging from 3.0 to 6.0, citrate buffer was used. For pH 7.0–9.0, Tris buffer was used. For pH 10.0 carbonate/bicarbonate buffer was used. The color development reaction with DNS was done exactly as for the temperature scans above. The highest activity obtained was considered to be 100% and the remaining activities were converted into percentage values of the maximum activity observed.

2.6. Structure determination, analysis and representation

The structure of MT Cel12A was determined by X-ray crystallography, using the standard technique of molecular replacement. For this, concentrated MT Cel12A (9.0 mg/ml) in 10 mM Tris, pH 7.5 was used as the protein stock solution. Crystals were grown by the hanging drop method using 0.2 M $NaH_2PO_4{\cdot}H_2O$; 20% PEG 3350 and pH 4.5 as reservoir solution. Protein stock was mixed with an equal volume of reservoir solution and equilibrated against the same buffer. Crystals grew within 3 to 4 days at 20 °C (Supplementary Fig. S7). X-ray diffracted intensity data were collected using a mar345 image plate detector mounted on a rotating anode generator (Rigaku Ultrax 18 model) through mounting of a crystal in a capillary tube at 25 °C. A total of 90 frames each with 1° oscillation were collected. Data were indexed and scaled using the *automar v1.10.6* suite of programs. The crystal showed a P212121 space group, with four molecules per asymmetric unit. The structure was determined by molecular replacement with RM Cel12A serving as a model (pdb entry 1H0B) and using *molrep* software as implemented in the CCP4 suite. Model building was performed by using the program *coot*, and the structure was refined by using *refmac*. Further details are available in Supplementary Table S7. The structure has been deposited in the PDB with the accession code, 3B7 M, and made accessible. The softwares *InSight II (Accelrys)* and *PYMOL* [23] were used for structure visualization, and *PYMOL* was used to produce the figures published in this paper.

3. Results and discussion

We carried out: (1) a detailed analysis of the superimposability of TR Cel12A and RM Cel12A, using the software LSQMAN [21] to identify all pairs of analogous residues occupying structurally-analogous positions in the two enzymes (Supplementary Table S1). Then, we identified (2) the subset of residues with C_α atoms located in strands and loops participating in the formation of the floor and walls of the cellulose-binding groove (Supplementary Table S2). Subsequently, we separated (3) the above subset into residues with sidechains facing into the groove, and away from the groove (Supplementary Table S3). Finally, (4) we excluded all residue pairs with sidechains facing away from the groove, to generate a final list of sidechains contributing directly to groove formation in both the enzymes, or in TR Cel12A with no counterpart in RM Cel12A (Supplementary Table S4). This list also helped identify which groove-forming sidechains are conserved, to help determine which ones have to be mutated to effect a replacement of the RM Cel12A groove by the TR Cel12A groove. The groove was found to be formed by a total of 66 residues in RM Cel12A, and 57 residues in TR Cel12A; the difference in numbers owing to differences in loop sizes. About 29 residues from TR Cel12A were represented by non-identical, structurally-analogous counterparts in RM Cel12A. Two loops (Cys66–Leu77 and Ser115–Gly118) in RM Cel12A were found to have been replaced in TR Cel12A by non-superimposable loops of 3 residues each (Ile67–Gln69 and His108–Thr110). Further, there was one insertion (Ala153) in TR Cel12A between positions corresponding to Asp160 and Trp161 in RM Cel12A. Details of mutated and conserved residues can be seen in a structure-based sequence alignment (Fig. 1B).

The designed RM Cel12A variant bearing the graft from TR Cel12A, named MT Cel12A (for mesoactive–thermostable Cel12A), was produced in *E. coli* in fusion with an N-terminal 6xHis affinity tag. Affinity-purified MT Cel12A was characterized and its structure determined through X-ray crystallography (see Supplementary Figs.S4–S7, Supplementary Table S7 and PDB accession code 3B7 M). The enzyme crystallized as a tetramer (Fig. 1C), unlike RM Cel12A which is a dimer [17], or TR Cel12A which is a hexamer [16]. One loop exists in two conformations in MT Cel12A, with two subunits of the tetramer adopting one conformation, and the other two subunits the other conformation (Fig. 1D).

A detailed comparison of MT Cel12A, RM Cel12A, and TR Cel12A, reveals a remarkable superimposability of backbone amongst all three structures, establishing that the surface graft did not affect folding. In the loops and strands of the groove region, the backbone of MT Cel12A is more superimposable with that of TR Cel12A, while in other regions it is more superimposable with that of RM Cel12A (Fig. 1A). As for the surface features of the three structures, the groove region of MT Cel12A (Fig. 2B) can be clearly seen to resemble that of TR Cel12A (Fig. 2C) and not RM Cel12A (Fig. 2A), whereas the opposite is true for

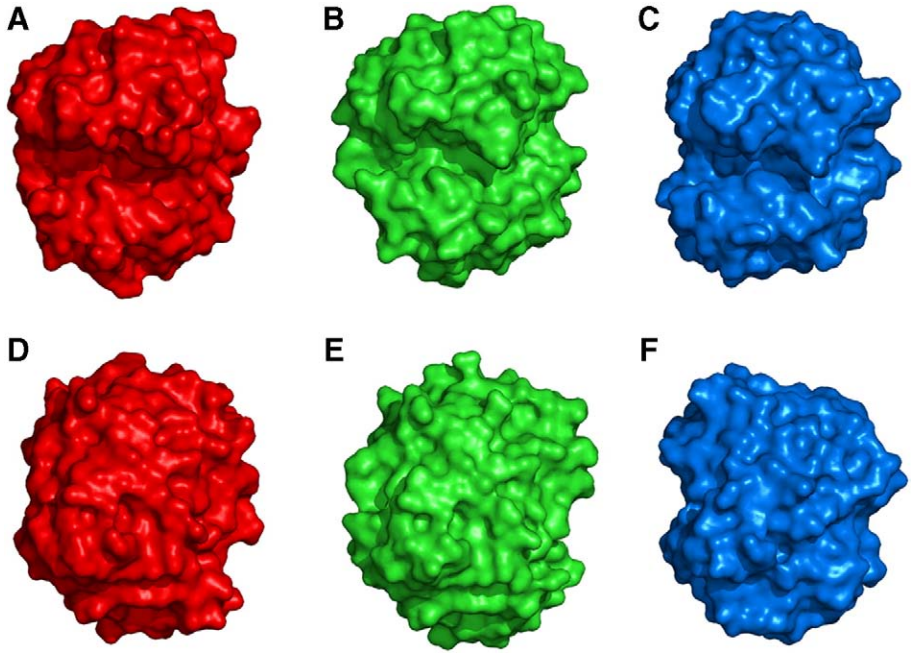

Fig. 2. Microstructural features of the top (groove) and bottom surfaces of RM Cel12A, MT Cel12A and TR Cel12A. Panels A, B and C, respectively, show top (groove) views of RM Cel12A, MT Cel12A and TR Cel12A, viewed from the same perspective after superimposition of backbones. Likewise, Panels D, E and F, respectively, show bottom views of RM Cel12A, MT Cel12A and TR Cel12A, i.e., the surfaces diametrically opposite the grooves on the other side of each enzyme.

the bottom surface of MT Cel12A which resembles RM Cel12A, and not the TR Cel12A progenitor (Figs. 2D–F). A side-view representation is shown to highlight the 36 TR Cel12A sidechains grafted onto RM Cel12A while creating MT Cel12A (Fig. 3A), together with all ~60 residues (including conserved sidechains) effectively involved in creating the grafted surface (Fig. 3B); comparing Fig. 3A and B, it may be noted that residues constituting one wall of the groove were highly conserved between RM Cel12A and TR Cel12A, causing replacements to be mainly required on the opposite wall, suggesting that the latter's residues could be primarily responsible for the differences in T_{opt}.

In conformity with crystal structure data, circular dichroism (CD) spectroscopy establishes that MT Cel12A adopts a predominantly beta sheet structure (Fig. 3C), similar to that of RM Cel12A (see Supplementary Fig.S8). Thermal stability was assessed by monitoring changes in mean residue ellipticity (MRE) at 217 nm (Fig. 3D) as a function of temperature. Melting was found to be initiated only above 85 °C, with only 20% unfolding even at 98 °C, establishing that the T_m of MT Cel12A is like that of RM Cel12A (see Supplementary Fig.S9E), which is reported to have a $T_m \gg 90$ °C [17], and entirely unlike that of TR Cel12A (see Supplementary Fig. S9F) which is reported to have a T_m of ~54 °C [20]. This conservation of stability, in all likelihood, owes to the deliberate avoidance of mutations of interior-facing residues.

Measurement of total activity as a function of temperature (Fig. 3E) showed that the T_{opt} of MT Cel12A is ~55 °C, suggesting that it derives its T_{opt} from TR Cel12A (see Supplementary Fig. S9B) which is reported to have a T_{opt} of ~50 °C [18], rather than from RM Cel12A (see Supplementary Fig. S9A), which has a T_{opt} of >90 °C [19]. We also measured the pH optimum of activity (pH_{opt}) of MT Cel12A which was found to be 6.0 (Fig. 3F); this pH_{opt} is not like that of TR Cel12A (see Supplementary Fig. S9D) but rather equally distinct from the values of ~5.0, and ~6.0–7.0, respectively, reported for TR Cel12A [18], and RM Cel12A (see Supplementary Fig. S9C) [24]. We would like to mention that the total activity of MT Cel12A was five-fold lower at 50 °C and pH 5.0 than that of RM Cel12A.

We appear to have dissected and reassorted T_{opt} and T_m values by creating an enzyme with a T_{opt} of 55 °C, and a $T_m \gg 90$ °C. The temperature *vs* activity profile of MT Cel12A is broader than that reported for TR Cel12A (see Supplementary Fig. S9B) [18], owing presumably to the fact that there is no longer a sharp cooperative melting at 54 °C, as was the case previously with the TR Cel12A structure [20]. What our work shows, therefore, is (a) that the active surface of TR Cel12A was evolved to function optimally at ~50 °C, (b) that it continues to do so, even after transfer to a more thermostable enzyme, and (c) that it is capable, however, of working sub-optimally at temperatures higher than 54 °C when afforded the opportunity to do so, by a stable structural scaffold. This suggests that the generally observed correlation between the temperature of optimal function of any enzyme and its thermal melting temperature could be an incidental fact of nature, involving only a coevolution of conformational stability and protein surface residue flexibilities, rather than any mandatory coupling of activity and stability behavior. We have demonstrated that the response to temperature of a group of interacting non-contiguous sidechains coming together on a protein's surface can be quite autonomous of the temperature-response of the structural scaffold that presents that surface. We have shown that an enzyme active surface that has evolved to become destabilized at high temperatures can retain its original mesophile functionality to a substantial extent, without necessarily taking complete advantage of the presence of a thermophile structural scaffold to raise its temperature of optimal function to thermophile levels. This indicates that enzyme inactivation at high temperatures might owe as much to the microconformational instability of the active surface, as to the macroconformational instability of the overall polypeptide fold. Of course, it may be appreciated the autonomy of stability and activity that we've demonstrated can only be exploited through transplantation experiments placing mesophile active surfaces on thermophile structural scaffolds, and not the other way around, since obviously a poorly stable scaffold could not be expected to support or sustain a highly stable, thermophile active surface, pre-evolved to work at very high temperatures. Even so, our work opens up novel avenues for much creative segregation and independent assortment of activity and stability characteristics between homologous proteins from different domains of life, for the creation of enzymes that nature would not ordinarily produce.

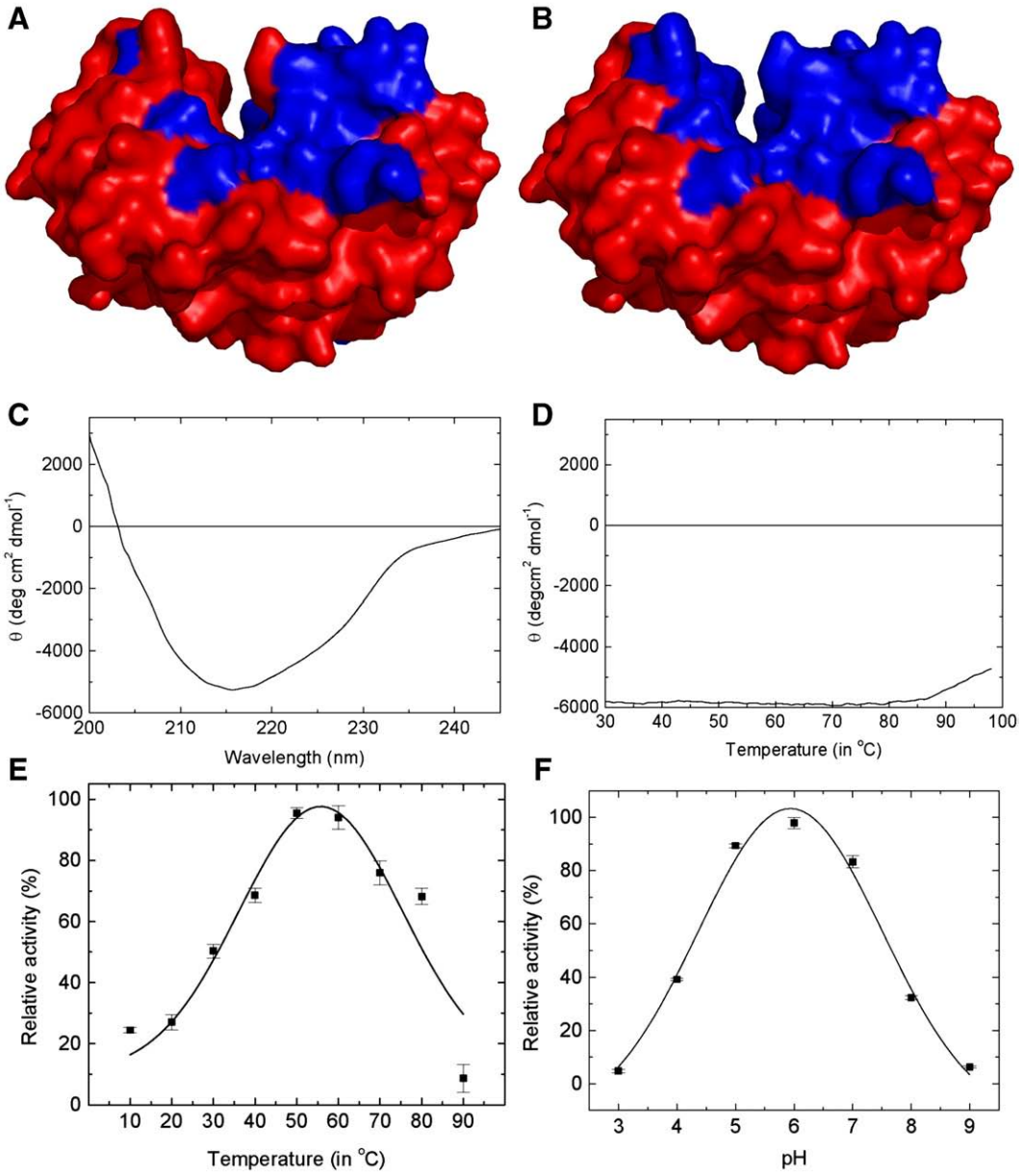

Fig. 3. Details and characteristics of the skin-graft bearing MT Cel12A. Panel A. A side-view surface representation of MT Cel12A, showing residues derived from RM Cel12A (in red), as well as 36 residues imported from TR Cel12A (in blue), following various substitutions, insertions or deletions as detailed in Fig. 1B. Panel B. A side-view surface representation of MT Cel12A, showing all groove residues effectively comprising the skin-graft. Note that groove residues conserved between RM Cel12A and TR Cel12A, genetically derived from RM Cel12A (shown in red in panel A) are shown here in blue. Panel C. Far-UV CD spectrum of MT Cel12A. Panel D. Far-UV MRE signal of MT Cel12A at 217 nm, as a function of increasing temperature. Panel E. Activity-*vs*-temperature profile of MT Cel12A collected at pH 5.0. Panel F. Activity-*vs*-pH profile of MT Cel12A collected at 50 °C. Error bars in panels E and F show standard error calculated for 5 independent observations each.

Notably, the possibility that enzyme active surfaces may be autonomous of their structural scaffold has previously been noted in denaturant-unfolding experiments reporting destruction of activity under milder conditions that those required to cause unfolding [25]. We tested the inactivation and denaturation of MT Cel12A, and RM Cel12A, by the chaotropic agent, guanidium hydrochloride (Gdm·HCl), to check whether the separation of the chemical inactivation and denaturation profiles is more profound in MT Cel12A than in RM Cel12A, as observed for the separation of the thermal inactivation and denaturation profiles. Indeed, the sensitivity to Gdm·HCl-inactivation of MT Cel12A was dramatically-higher than that of RM Cel12A, whereas the sensitivity of MT Cel12A to Gdm·HCl-denaturation was only marginally higher than that of RM Cel12A (see Supplementary Fig. S10).

Given the systematicity and rationale of the residue-replacement approach that we have developed and used for the active surface transplantation experiment reported in this paper, we would propose that this approach would be likely to work with virtually any beta sheet structure-based enzyme, although, of course, just as all previous engineering approaches have been characterized by both success and failure, this approach too might fail in certain instances. Our objective in performing and presenting this work has been to encourage others to try the same approach, whenever a need is perceived to mix-and-match the characteristics of two homologous proteins to derive a novel protein differentially combining the interior and surface features of these proteins.

Acknowledgements

DK, VK, SKC, SA, SS, and MD thank the CSIR, New Delhi, for research fellowships. BV, KS and PG thank the CSIR, the DBT and INSA for grants

supporting research in protein structural bioinformatics, structural biology, biophysics and biochemistry.

Appendix A. Supplementary data

Supplementary data associated with this article can be found, in the online version, at doi:10.1016/j.bbapap.2008.05.007.

References

[1] C.S. Craik, C. Largman, T. Fletcher, S. Roczniak, P.J. Barr, R. Fletterick, W.J. Rutter, Redesigning trypsin: alteration of substrate specificity, Science 228 (1985) 291–297.
[2] J.A. Wells, D.B. Powers, R.R. Bott, T.P. Graycar, D.A. Estell, Designing substrate specificity by protein engineering of electrostatic interactions, Proc. Natl. Acad. Sci. U. S. A. 84 (1987) 1219–1223.
[3] N.S. Scrutton, A. Berry, R.N. Perham, Redesign of the coenzyme specificity of a dehydrogenase by protein engineering, Nature 343 (1990) 38–43.
[4] A.E. Nixon, S.M. Firestine, F.J. Salinas, S.J. Benkovic, Rational design of a scytalone dehydratase-like enzyme using a structurally-homologous protein scaffold, Proc. Natl. Acad. Sci. U. S. A. 96 (1999) 3568–3571.
[5] M.A. Dwyer, L.L. Looger, H.W. Hellinga, Computational design of a biologically active enzyme, Science 304 (2004) 1916–1917.
[6] R.A. Chica, N. Doucet, J.N. Pelletier, Semi-rational approaches to engineering enzyme activity: combining the benefits of directed evolution and rational design, Curr. Opin. Biotechnol. 16 (2005) 378–384.
[7] Z. Chen, H. Zhao, Rapid creation of a novel protein function by in vitro coevolution, J. Mol. Biol. 348 (2005) 1273–1282.
[8] S.L. Strausberg, B. Ruan, K.E. Fisher, P.A. Alexander, P.N. Bryan, Directed coevolution of stability and catalytic activity in calcium free subtilisin, Biochemistry 44 (2005) 3272–3279.
[9] P. Acharya, E. Rajakumara, R. Sankaranarayanan, N.M. Rao, Structural basis of selection and thermostability of laboratory evolved *Bacillus subtilis* lipase. J. Mol. Biol. 341 (2004) 1271–1281.
[10] H.S. Park, S.H. Nam, J.K. Lee, C.N. Yoon, B. Mannervik, S.J. Benkovic, H.S. Kim, Design and evolution of new catalytic activity with an existing protein scaffold, Science 311 (2006) 535–538.
[11] M. Peimbert, L. Segovia, Evolutionary engineering of a beta-lactamase activity on a D-Ala D-Ala transpeptidase fold. Protein Eng. 16 (2003) 27–35.
[12] K. Chockalingam, A. Chen, J.A. Katzenellenbogen, H. Zhao, Directed evolution of specific receptor–ligand pairs for use in the creation of gene switches, Proc. Natl. Acad. Sci. U. S. A. 102 (2005) 5691–5696.
[13] A. Singh, K. Hayashi, Construction of chimeric beta glucosidases with improved enzymatic properties, J. Biol. Chem. 270 (1995) 21928–21933.
[14] M.A. Arnott, R.A. Michael, C.R. Thompson, D.W. Hough, M.J. Danson, Thermostability and thermoactivity of citrate synthases from the thermophilic and hyperthermophilic archaea, *Thermoplasma acidophilum* and *Pyrococcus furiosus*, J. Mol. Biol. 304 (2000) 657–668.
[15] K.L. Morley, R.J. Kazlauskas, Improving enzyme properties: when are closer mutations better? Trends Biotechnol. 23 (2005) 231–237.
[16] M. Sandgren, A. Shaw, T.H. Ropp, S. Wu, R. Bott, A.D. Cameron, J. Stahlberg, C. Mitchinson, T.A. Jones, The X-ray crystal structure of the *Trichoderma reesei* family 12 endoglucanase 3, Cel12A, at 1.9 Å resolution, J. Mol. Biol. 308 (2001) 295–310.
[17] S.J. Crennell, G.O. Hreggvidsson, E.N. Karlsson, The structure of *Rhodothermus marinus* Cel12A, a highly thermostable family 12 endoglucanse at 1.8 Å resolution, J. Mol. Biol. 320 (2002) 883–897.
[18] J. Karlsson, M. Siika-aho, M. Tenkanen, F. Tjerneld, Enzymatic properties of the low molecular mass endoglucanases Cel12A (EG III) and Cel45A (EG V) of *Trichoderma reesei*, J. Biotechnol. 99 (2002) 63–78.
[19] K.B. Wicher, M. Abou-Hachem, S. Halldorsdottir, S.H. Thorbjarnadottir, G. Eggertsson, G.O. Hreggvidsson, E.N. Karlsson, O. Holst, Deletion of a cytotoxic N-terminal putative signal peptide results in a significant increase in production yields in *Escherichia coli* and improved specific activity of Cel12A from *Rhodothermus marinus*, Appl. Microbiol. Biotechnol. 55 (2001) 578–584.
[20] M. Sandgren, P.J. Gualfetti, A. Shaw, L.S. Gross, M. Saldajeno, A.G. Day, T.A. Jones, C. Mitchinson, Comparison of family 12 glycoside hydrolases and recruited substitutions important for thermal stability, Protein Sci. 12 (2003) 848–860.
[21] G.J. Kleywegt, Use of non-crystallographic symmetry in protein structure refinement, Acta Crystallogr. Sect. D 52 (1996) 842–857.
[22] G.L. Miller, R. Blum, W.E. Glennon, A.L. Burton, Measurement of carboxymethyl cellulase activity, Anal. Biochem. 2 (1960) 127–132.
[23] W.L. DeLano, The PyMOL User's Manual, DeLano Scientific, Palo Alto, CA, USA, 2002.
[24] S. Halldorsdottir, E.T. Thorolfsdottir, R. Spilliaert, M. Johansson, S.H. Thorbjarnadottir, A. Palsdottir, G.O. Hreggvidsson, J.K. Kristjansson, O. Holst, G. Eggertsson, Cloning, sequencing and overexpression of a *Rhodothermus marinus* gene encoding a thermostable cellulase of glycosyl hydrolase family 12, Appl. Microbiol. Biotechnol. 49 (1998) 277–284.
[25] C.L. Tsou, Conformational flexibility of enzyme active sites, Science 262 (1993) 380–381.